Early View publication on www.interscience.wiley.com
(issue and page numbers not yet assigned;
citable using Digital Object Identifier – **DOI**)

phys. stat. sol. (b), 1–5 (2008) / **DOI** 10.1002/pssb.200743443

physica status solidi b
www.pss-b.com
basic solid state physics

Coarse-grained modelling of polypyrrole morphologies

Victor Rühle[1], James Kirkpatrick[1,2], Kurt Kremer[1], and Denis Andrienko[*,1]

[1] Max Planck Institut für Polymerforschung, Ackermannweg 10, 55128 Mainz, Germany
[2] Centre for Electronic Materials and Devices, Department of Physics, Imperial College London, London SW7 2BW, UK

Received 22 October 2007, revised 5 December 2007, accepted 14 December 2007
Published online 1 February 2008

PACS 36.20.Ey, 68.55.J–, 73.61.Ph, 82.35.Lr

[*] Corresponding author: e-mail denis.andrienko@mpip-mainz.mpg.de

A multiscale model to simulate large scale morphologies and study charge transport in polypyrrole is developed. First, *ab-initio* methods are used to derive an atomistic force field. Coarse graining of this atomistic model is then performed. At a final stage, the analysis of simulated morphologies allows to split polymer chains into conjugated segments, which can further be used to simulate both inter- and intrachain charge dynamics.

1 Introduction Historically, polypyrrole is probably the very first polymer reported to have good conducting properties when oxidized [1]. It is easy to synthesize and handle; conductivities up to 300 S cm^{-1} were reported in the oxidized state. The structure and therefore the conductivity of polypyrrole heavily depends on the processing. The extreme insolubility of polypyrrole in organic solvents hinders detailed structural analysis. Therefore, much about the physical properties and structural characteristics is not well understood and reports are often contradictory [2]. An experimental overview of electrochemistry of conducting polypyrrole films is given in Ref. [3]. Here we mention only the main and rather sparse theoretical contributions to the field.

The effect of doping on the geometric and electronic structure has been studied in pioneering works of Brédas et al. [4, 5]. It was shown that for high doping levels bipolaron bands are formed, confirming experimental observations of the spinless nature of charge carriers in the highly doped state. Similar analysis was performed using density functional approaches [6, 7]. The hopping transport picture and underlying parameters were analysed for pyrrole oligomers by Hutchison et al. [8]. The stability of oligomeric PPy structures bonded through α and β carbons was studied by Yutsever. It was shown that PPy is able to form branch like structures [9, 10].

At the atomistic level of description, OPLS-AA force field parameters were derived for liquid pyrrole by Jorgensen et al. [11]. Molecular dynamics (MD) simulations of solvated reduced and oxidized polypyrrole were performed by Cascales et al. [12, 13]. In these simulations, the standard GROMOS torsion potential connecting repeat units was used for the neutral as well as the doped polymer. Apart from the fact that this potential contradicts recent quantum-chemical calculations [14], in what follows we show that it differs significantly for doped and oxidized states.

Hence, the first important task on the way of modelling large-scale PPy morphologies is the development of a reliable atomistic force field, with appropriate parameters for the torsion potential and correct partial charge distributions in reduced and oxidized states. This is the first part of this work. Our final aim is, of course, to relate conductivity/charge mobility to the underlying morphology. This is a true multiscale problem: local hopping rates for charge carriers are very sensitive to specific chemistry and local conformations. At the same time, such macroscopic properties as mobility and conductivity depend on the path a charge takes and therefore on the large scale morphology of the whole sample. However, these morphologies cannot be obtained using standard atomistic molecular dynamics due to limitations imposed by equilibration times as well as system size. A coarse-graining technique which remedies the situation is the topic of the second part of this contribution. Finally we discuss our future plan for modelling charge transport in the simulated morphologies. The transport model we utilise is temperature activated polaron hopping,

as described in non-adiabatic high-temperature Marcus theory.

2 Atomistic model Our first step is to set up a reliable atomistic model of PPy. As a starting point, we used the OPLS-AA force field, which is based on the force field parameters of pyrrole monomers [11]. The parameters of the dihedral and improper potentials connecting repeat units are of course not available in the standard force field. *Ab-initio* calculations were performed to derive them. In what follows, we describe the procedure for the dihedral potential; the improper potential, which keeps the bond connecting two adjacent repeat units in their planes, was obtained in a similar way.

The torsion angle θ of the N–C–C–N dihedral in 2,2′-bipyrrole (see Fig. 1) was scanned and the torsion potential was evaluated using B3LYP hybrid density functional and 6-311++G(3df,3pd) basis set. Calculations were performed using GAUSSIAN package [15]. At each scanning step, the dihedral angle θ was fixed at the value of interest while the rest of the structure was optimized. The dependence of the potential on the torsion angle is depicted in Fig. 1. To obtain the parameters of the dihedral potential from the *ab-initio* potential energy, we took the optimized geometries and let them further relax in MD, again constraining the dihedral angle and with its parameters set to zero. The force-field based potential energy of these relaxed contributions was then subtracted from the potential energy curve provided by *ab-initio* calculations. Note that the direct fitting, without the subtraction, is a common mistake which leads to a double counting of those energy contributions already taken care of in the existing atomistic model, such as bond, angle, improper dihedral, Coulomb and Lennard-Jones interaction potentials. Another, more subtle problem is that the minimum energy conformation in the atomistic model has small deviations compared to the quantum chemically optimized structures. To avoid this mismatch the *ab-initio* structures are relaxed in MD with the constraints imposed during the *ab-initio* optimization.

Table 1 Fitted values for the N–C–C–N Ryckaerd–Belleman dihedral connecting two repeat units. All values are given in kJ/mol.

C_0	C_1	C_2	C_3	C_4	C_5
16.039	−2.483	−25.859	3.302	11.034	−2.184

The relaxation in MD leads to barriers of equal heights both in quantum chemical and atomistic simulations. Without relaxation internal stresses (mainly due to improper dihedrals) would lead to lower barriers. Charges were calculated using B3LYP/6-311G(d,p) and CHELPG [16] fitting procedure in a chain of 8 repeat units.

A Ryckaerd–Belleman type potential was used to fit the potential energy difference

$$V_{\mathrm{rb}} = \sum_{n=0}^{5} C_n (\cos\theta)^n . \tag{1}$$

The fitted values are given in Table 1.

We shall also comment on the accuracy of DFT: Even though DFT does not show perfect agreement with higher correlated quantum chemical methods when applied to judging rotational barriers in conjugated materials [17], we judge that its accuracy is still sufficient in the case of polypyrrole [14], given the other errors introduced in atomistic simulation.

To study the effect of doping on the force field parameters, we scanned the torsion angle of a charged chain. Since the best conductivities are obtained for a doping rate of one charge per three repeat units [18], we used a charged tetramer and scanned around the middle dihedral. Figure 2 shows the potential energy of the neutral and the charged tetramer. It is clear that the barrier is increased and the planar configuration is favored when the polymer is doped. This high barrier cannot be reproduced by the previously used atomistic models, even if the charges are adjusted to the doped case. Moreover, for a doped polymer, partial charges of the atoms do not increase homogene-

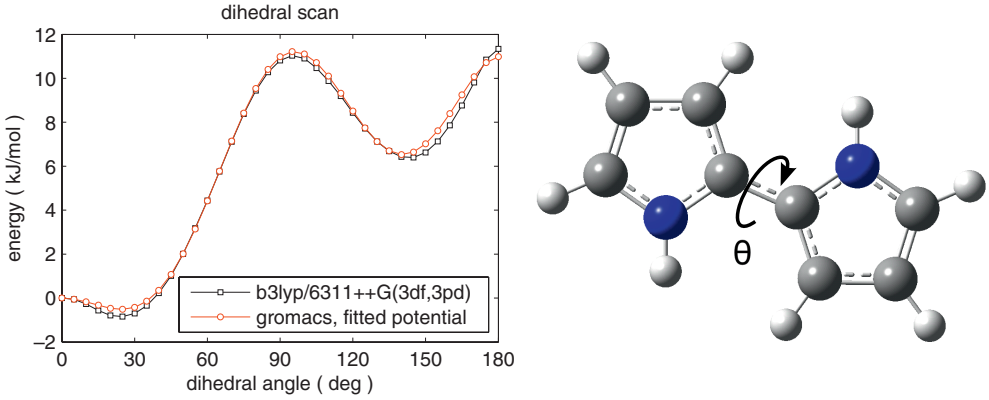

Figure 1 (online colour at: www.pss-b.com) Potential energy curve for a 2,2′-bipyrrole as a function of the dihedral angle θ. Squares: density functional data, B3LYP/6-311++G(3df,3pd). Circles: fitted dihedral potential with the rest of the parameters taken from the OPLS-AA force field.

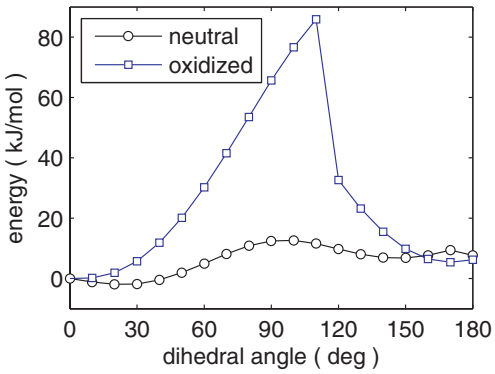

Figure 2 (online colour at: www.pss-b.com) Energies, when a pyrrole tetramer is rotated around the middle bond, are compared in the undoped (black line) and doped (blue line) case.

ously: the whole distribution along the chain changes. Hence, both the dihedral potential and partial charges should be adjusted in order to correctly describe doped chains. The chemical reason for the increase of planarity in PPY upon doping is the quinoid structure of oxidized PPY, i.e. double bond character of the bond connecting successive monomers. When an oxidized oligomer is forced to aquire a twisted conformation the molecule will find itself in a diradical state which cannot be properly described by ground state theories such as DFT. Having said this, it is also clear that small deviation from planarity (where diradical formation can be assumed not to play an important role) results in much larger potential energies in the oxidized than in the reduced states: DFT cannot give correct quantitative estimates of the rotational barrier in charged PPY but can certainly describe the general trends: a reduction in bond length of the inter-monomer bond and a massive increase in stiffness.

3 Coarse graining Atomistic simulations are limited to a small number of atoms and/or short timescales. To

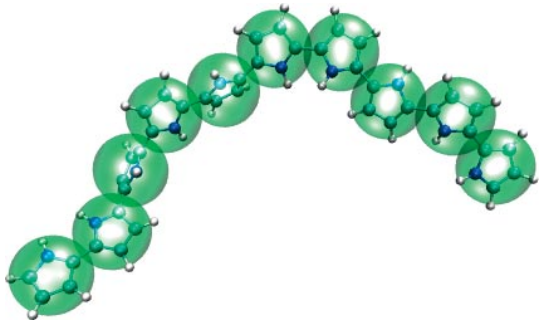

Figure 3 (online colour at: www.pss-b.com) Mapping scheme for PPy. On the coarse grained level, each monomer is described by one bead (green spheres). The beads are connected by bond, angle and dihedral potentials.

overcome these limitations, various coarse graining techniques were developed over the past years [19–25]. The idea of coarse graining is to integrate out as many degrees of freedom as possible while still being able to reproduce the important properties of the system.

Here we follow the idea of Tschöp et al. [21]. The model averages out all fast internal degrees of freedom by mapping groups of atoms to coarse grained beads. For the polypyrrole, we use a 1:1 mapping scheme where one chemical repeat unit is mapped onto one bead (see Fig. 3). Centers of mass of repeat units without the hydrogens were used as centers of the beads. Beads are connected by bond, angle and dihedral potentials. Coarse grained potentials were derived using the inverse Boltzmann method [21]. Phase space was sampled by a stochastic dynamics simulation of an isolated atomistic chain in vacuum. Thus the distribution of states is in the canonical ensemble. All non-bonded interactions that correspond to 1–5 or further interactions in the coarse grained scheme were excluded. Closer non-bonded interactions were considered since they are a part of the bonded interactions in the coarse grained model.

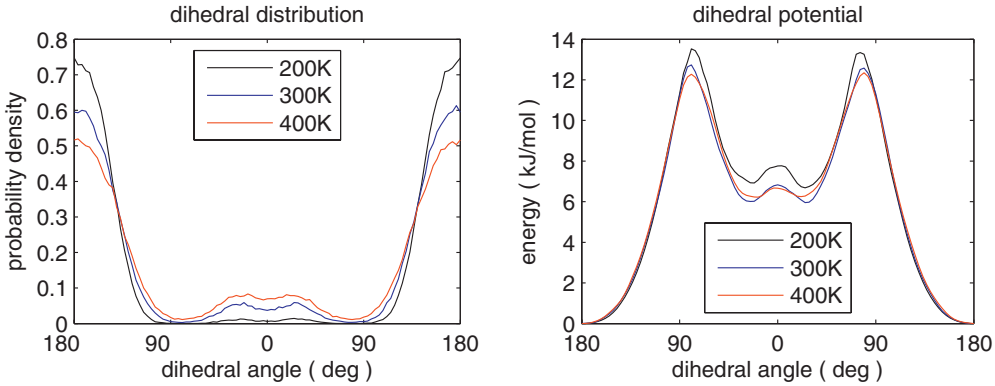

Figure 4 (online colour at: www.pss-b.com) Probability distribution (left) and potential (right) for the dihedral potential that connects the beads in the coarse grained model is plotted at 200 K (black), 300 K (blue) and 400 K (red). The potential was calculated by Boltzmann inverting the probability distribution followed by a smoothing step to filter noise. With increasing temperature, the probability distribution broadens but the corresponding potentials do not change much. This fact is not compulsory since entropic contributions can, in principle, change the potential and are temperature dependent.

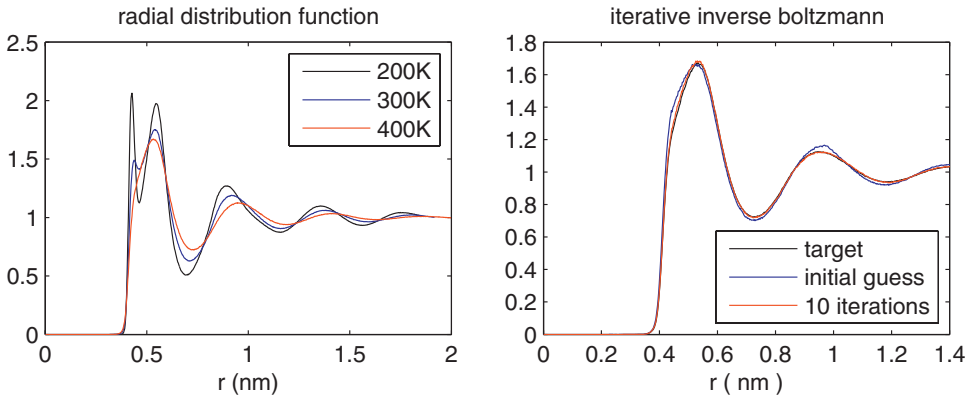

Figure 5 (online colour at: www.pss-b.com) Left: radial distribution functions of an atomistic melt of monomers mapped onto coarse grained beads for 200 K, 300 K and 400 K. Right: the radial distribution function at 400 K was fitted to the coarse grained model using iterative Boltzmann method. Good agreement was achieved after 10 iterations.

The coarse grained conformations with the yet unknown potentials also sample a canonical distribution, and are thus Boltzmann distributed. Assuming that the bonds, angles and dihedrals are independent and factorize, i.e.

$$P(r,\varphi,\theta) = P(r)\,P(\varphi)\,P(\theta)\,, \tag{2}$$

their potentials can be calculated separately by inverting the Boltzmann distribution

$$U(r) = -k_{\mathrm{B}}T\,\ln P(r)\,, \qquad U(\varphi) = -k_{\mathrm{B}}T\,\ln P(\varphi)\,,$$

$$U(\theta) = -k_{\mathrm{B}}T\,\ln P(\theta)\,. \tag{3}$$

The distributions and Boltzmann inverted potentials of the dihedral are plotted for different temperatures in Fig. 4.

Analyzing the distributions we found that in the coarse grained model bonds are very stiff; to a good approximation one can use constrained bonds of length 0.377 nm. The angle potential was fitted with a harmonic potential ($\varphi_0 = 140$ deg, $k = 600$ kJ/mol/rad^2) while tabulated potentials were used for the coarse grained dihedral potential. All values were derived at 300 K.

To calculate the non-bonded potentials, the iterative inverse Boltzmann method (IBM) [20, 24] was used to match the radial distribution function (rdf) of liquid pyrrole. Rdfs were calculated based on trajectories of atomistic MD simulations at different temperatures. A box of 512 pyrrole monomers was first equilibrated in a NPT run (Berendsen thermo- and barostat) at 1 bar and 200 K, 300 K and 400 K followed by a production run in the NVT ensemble. Monomers were mapped to coarse grained beads and the rdfs were calculated. The rdfs, which are shown in Fig. 5, reflect the ellipsoid-like shape of the pyrrole monomers: at 400 K, the first peak is slightly deformed. With decreasing temperature, this peak splits up into two smaller peaks, due to differend relative orientations of neighboring monomers.

Based on the rdfs, the coarse grained potentials can be derived iteratively. A reasonable initial guess is the Boltzmann inverted radial distribution function

$$U_{\mathrm{AA}}(r) = -k_{\mathrm{B}}T\,\ln g(r)\,. \tag{4}$$

However, this expression is exact only in the limit of an infinitely dilute system, but can be used as a starting point to iteratively improve the potential of coarse-grained beads

$$U_{i+1}(r) = U_i(r) + k_{\mathrm{B}}T\,\ln\frac{g_i(r)}{g(r)} \tag{5}$$

till convergence is reached. Figure 5 compares the radial distribution function obtained using the initial guess, the rdf after 10 iterations, and the target rdf. Note that this method can be used to derive non-bonded potentials for pyrrole monomers and in principle one has to study a set of oligomers to account for connectivity effects. This work is in progress.

To summarize, we have developed a coarse-grained model which can be used to study large-scale morphologies of PPy. Generated morphologies will, of course, describe correctly only the global conformations of mesophases, due to intrinsic approximations of coarse-graining. However, the coarse grained morphology can be mapped back to atomistic resolution. Followed by a short atomistic equilibration it will allow for large scale morphologies with atomistic level of details [26], suitable for studying charge transport in PPy.

4 Outlook The aim of this work is to model charge mobilities and conductivity in polypyrrole. The context within which we will work is that of temperature activated polaron hopping, as described in non-adiabatic high-temperature Marcus theory. In this model charge hopping rates are determined by three parameters: the reorganization energy (a measure of the polaron localization energy), the transfer integral (a measure of the strength of electronic coupling) and finally the difference in free energies before and after charge hops. One of the fundamental assumptions underlying non-adiabatic theory is that the polaron local-

ization energy, that is the energy gained in localizing a charge, is smaller than the electronic coupling. This is probably always true for intermolecular hops in a conjugated polymer, but is most certainly not true in the case of intramolecular hops. For this purpose we propose to segment the polymer into conjugated segments and consider those as our charge transporting units. The reorganization energy [8] and site energy will then primarily depend on the spatial extension of the conjugated segment, whereas the electronic coupling will primarily depend on the molecular overlap between adjacent conjugated segments. Several potential difficulties will be considered: coarse grained simulations will be used to determine the timescale on which conjugated segments change length. We will also consider the influence of the change in stiffness of torsional potentials upon charge dynamics. Another issue to be investigated is the role of bipolarons [4, 5] in hopping, while it is known that doubly charged spinless excitations are involved in the charge transport it is not yet clear how these excitations travel: do they hop "at once" or in two stages?

Having determined charge transport parameters, mobility can be simulated using numerical techniques such as kinetic Monte Carlo or by solving the Master Equation for charge hopping.

Acknowledgements This work was partially supported by DFG. J.K. acknowledges the EPSRC. Discussions with G. Wegner, K. Lienkamp, and J. Wang are gratefully acknowledged. All atomistic simulations in this work were done using GROMACS [27]. Berk Hess is acknowledged for providing many advises related to this simulation package.

References

[1] B. A. Bolto, R. McNeill, and D. E. Weiss, Aust. J. Chem. **16**, 1090 (1963).
[2] K. Lienkamp and G. Wegner, Macromol. Rapid Commun. **28**, 1112 (2007).
[3] A. F. Diaz, J. I. Castillo, J. A. Logan, and W. Y. Lee, J. Electroanal. Chem. **129**, 115 (1981).
[4] J. L. Brédas, B. Thémans, and J. M. André, Phys. Rev. B **27**, 7827 (1983).
[5] J. L. Brédas, B. Thémans, J. G. Fripiat, and J. M. André, Phys. Rev. B **29**, 6761 (1984).
[6] R. Colle and A. Curioni, J. Am. Chem. Soc. **120**, 4832 (1998).
[7] R. Colle and A. Curioni, J. Phys. Chem. A **104**, 8546 (2000).
[8] G. R. Hutchison, M. A. Ratner, and T. J. Marks, J. Am. Chem. Soc. **127**, 2339 (2005).
[9] M. Yurtsever and E. Yurtsever, Synth. Met. **98**, 221 (1999).
[10] E. Yurtsever, Okan Esentürk, H. Önder Pamuk, and M. Yurtsever, Synth. Met. **98**, 229 (1999).
[11] N. A. McDonald and W. L. Jorgensen, J. Phys. Chem. B **102**, 8049 (1998).
[12] J. J. López Cascales and T. F. Otero, J. Chem. Phys. **120**, 1951 (2005).
[13] J. J. López Cascales and T. F. Otero, Macromol. Theory Simul. **14**, 40–48 (2005).
[14] J. C. Sancho-Garci and A. Karpfen, Chem. Phys. Lett. **411**, 321 (2005).
[15] M. J. Frisch et al., Gaussian 03, Revision B.03 (Gaussian, Inc., Wallingford CT, 2004).
[16] C. M. Breneman and K. B. Wiberg, J. Comput. Chem. **11**, 361 (1990).
[17] B. Mannfors, J. T. Koskinen, L.-O. Pietilä, and L. Ahjopalo, J. Mol. Struct. (Theochem) **393**, 39 (1997).
[18] W. A. Goedel, G. Hölz, and G. Wegner, Polymer **34**, 4341 (1993).
[19] A. P. Lyubartsev and A. Laaksonen, Phys. Rev. E **52**, 3730 (1995).
[20] A. K. Soper, Chem. Phys. **202**, 295 (1996).
[21] W. Tschöp, K. Kremer, J. Batoulis, T. Bürger, and O. Hahn, Acta Polym. **49**, 61 (1998).
[22] F. Müller-Plathe, Chem. Phys. Chem. **3**, 754 (2002).
[23] C. F. Abrams and K. Kremer, Macromolecules **36**, 260 (2003).
[24] D. Reith, M. Pütz, and F. Müller-Plathe, J. Comput. Chem. **24**, 1624 (2003).
[25] S. Izvekov and G. A. Voth, J. Chem. Phys. **123**, 134105 (2005).
[26] W. Tschöp, K. Kremer, O. Hahn, J. Batoulis, and T. Bürger, Acta Polym. **49**, 75 (1998).
[27] D. van der Spoel, E. Lindahl, B. Hess, G. Groenhof, A. E. Mark, and H. J. C. Berendsen, J. Comput. Chem. **26**, 1701 (2005).